



Intraosseous ultrasound for assessment of pedicle screw holes in the thoracolumbar spine based on endoscopic ultrasound: An experimental study

Yun Dong^{1,2} · XiongXiong Zuo³ · HaiTao Sun^{4,5} · He Wang² · ShaoHui He⁴ · JianRu Xiao⁴ · XiaoPan Cai⁴

Received: 16 February 2025 / Accepted: 23 April 2025
© The Author(s) 2025

Abstract

Purpose Experimental assessment of the efficiency of intraosseous ultrasound (IOUS) utilizing the mini probe of endoscopic ultrasound (EUS) is performed to determine the accuracy of pedicle screw hole placements in thoracolumbar spine.

Methods Drill holes in 76 pedicles of thoracolumbar spines from 2 cases of goats. Each pedicle screw hole is subjected to a 360° circumferential IOUS scanning with a catheter-type mini ultrasound probe of EUS and to a CT examination. Subsequently, all ultrasound images were independently interpreted by 3 reviewers without knowledge of the real position of screw holes and the results of the CT examination for the assessment of screw hole malposition and pedicle cortex breach. Finally, according to the conclusion of CT, a Chi-square test is employed to assess the differences of interpretations of the screw hole malposition among the all reviewers and the relevant relationship between the recognition of the misplaced screw holes and imaging methods utilized.

Results CT revealed 13 correctly positioned holes and 63 holes deviating from correct position (including holes that penetrated the cortex). All ultrasound images with malposition identified by CT were correctly interpreted, with no false negatives and no intra-reviewer differences. There were no omissions of severe malposition (including the spinal canal was penetrated into). Excluding six false positives misjudged due to the intersection of screw holes on both sides, there was also no discrepancy between the EUS and CT imaging in the interpretation of screw hole malposition. The examination time of each pedicle screw hole with EUS took less than 15 s.

Conclusion EUS-based IOUS is an immediate, reliable and lower-cost technique for accurate determination of pedicle screw hole malposition. With a probe that is both flexible and not easily bendable, the EUS is particularly suitable for IOUS, especially in the narrow space of the bone gaps or bone canals, and minimally invasive spine surgery (MISS).

Keywords Intraosseous ultrasound · Endoscopic ultrasound · Pedicle screw hole · Malposition · Thoracolumbar spine

✉ JianRu Xiao
jianruxiao83@163.com

✉ XiaoPan Cai
caipan1982@163.com

¹ Department of Biomedical Engineering, School of Health Science and Engineering, University of Shanghai for Science and Technology, Shanghai, China

² Department of Ultrasonic Medicine, Shanghai East Hospital, Shanghai, China

³ Department of Medical Imaging, Shanghai East Hospital, Shanghai, China

⁴ Department of Orthopedics Oncology, Changzheng Hospital, Naval Medical University, Shanghai, China

⁵ Department of Spinal Surgery, Naval Hospital of Eastern Theater, Zhoushan, Zhejiang Province, China

Abbreviations

IOUS	Intraosseous ultrasound
EUS	Endoscopic ultrasound
MISS	Minimally invasive spine surgery
DSG	Dynamic surgical guidance
CBCT	Cone-beam CT
AR	Augmented reality
MR	Mixed reality
PI	Photoacoustic imaging
IVUS	Intravascular ultrasound
T	Thoracic vertebra
L	Lumbar vertebra
S	Sacral vertebra

Introduction

The cortical bone damage caused by misplaced pedicle screws can lead to various issues such as spinal instability or injury to surrounding tissues (including but not limited to blood vessels, nerves, and spinal cord, etc.) in patients [4]. The rates of surgical amendment and revision tend to augment as the number of implanted screws increases. In recent years, a variety of intraoperative techniques have been being developed to address the risk factors of screw misplacement, such as 3D printed patient-specific templates that requires less experience from surgeons [18], dynamic surgical guidance (DSG) that reduces the learning curve [1], cone-beam CT (CBCT) that accelerates data acquisition and 3D reconstruction [9], image-guided robot-assisted navigation system that decreases human errors and fatigues [14, 19], augmented or mixed reality (AR or MR) guidance technique that establishes a perspective effect combining virtual and real elements and provides feedback responses [2, 3, 5, 12], and photoacoustic imaging (PI) technique that is sensitive to minor changes in bone density and has better penetration capability [10, 17]. Despite the fact that these specific technologies show significant statistical benefits in reducing the rate of screw malposition compared to traditional, experience-dependent, free-hand screw placement methods still widely used by most surgeons today and promote a reduction in surgical time and radiation exposure, there is yet no consensus on which technology is superior among them. And most technologies still face the need for extensively exposed surgical fields, radiation exposure (even though the dose and duration have been reduced), lack of the rapid force feedback, high cost of technological equipment, insufficiency of efficient and high-speed big data computing power, and potential navigation failures due to intraoperative displacement of reference objects fixed on patients [16]. Currently, the above technologies have not demonstrated significant and robust benefits in clinical settings, nor have they been routinely applied in spinal fusion surgeries. Moreover, they all face the challenges posed by complex neuromuscular scoliosis.

IOUS is a general term for a new technology that directly monitors and assesses the integrity of bone channels and the properties of surrounding tissues during surgery by placing a miniature ultrasound probe within the natural or iatrogenic channels of the bone. This is a simple and easy-to-interpret technology that does not require additional personnel, extensive training, and complicated equipment [7]. Kantelhardt SR et al. reported and successfully validated the feasibility, sensitivity, and reliability of intravascular ultrasound (IVUS, a device for assessing the degree of coronary stenosis, with a frequency of 20 MHz

and a diameter of 1.2 mm) for intraoperative assessment of the positioning of pedicle screw holes in lumbar and lower cervical vertebrae in 2009 and 2010. The average examination time of IOUS using IVUS for every pedicle screw hole was no more than 1 min. And they believe that the design based on the catheter may be particularly suitable for percutaneous MISS [7, 8]. However, the bending of the flexible IVUS catheter may cause deformations of the 2D images of the screw holes and the distortions of 3D-reconstructed images. In addition, the high cost of disposable IVUS catheter has hindered in-depth research in the field of IOUS. Excitingly, the EUS probe has similar shape and physical properties (mini and elastic) as IVUS, and its tip is not easy to bend. This, combined with the lower cost and multiple use of EUS probes, has allowed the study of IOUS to continue. This research aims to achieve IOUS scanning by placing an EUS probe within the established pedicle screw holes in order to determinate the accuracy of pedicle screw hole placements and to evaluate the feasibility of this technique for clinical application and provide reliable experimental data to relevant researchers, engineers and medical device manufacturers.

Methods and materials

Preparation of experimental specimens

IOUS experiments utilizing EUS were performed on fresh thoracolumbar spine specimens from two goats (L1-S1). These specimens were all obtained from a legal local meat market. The cervical spine structure of quadruped is different from that of humans, hence, it is not suitable as a replacement for human cervical vertebrae. In contrast, the porcine and caprine thoracolumbar structures are similar to those of humans, and their sizes are close to those of humans, making them suitable alternatives for human thoracolumbar experiments. It is usually difficult to obtain entire porcine thoracolumbar spines from meat markets due to have been segmented by processing workshops before going to market. Relatively, influenced by regional dietary habits, most caprine thoracolumbar spines are manually separated to remain intact.

Preparation of the pedicle screw holes

The caprine thoracic spine consists of 13 vertebrae (T1-T13) and the lumbar spine consists of 6 vertebrae (L1-L6). Due to the vulnerability of T1 to damage and incompleteness when separated from the cervical spine, 76 pedicle screw holes with a diameter of 3 mm and a length of approximately 30–35 mm were prepared on both sides of the pedicles from T2 to S1 using a pneumatic drill (Fig. 1,

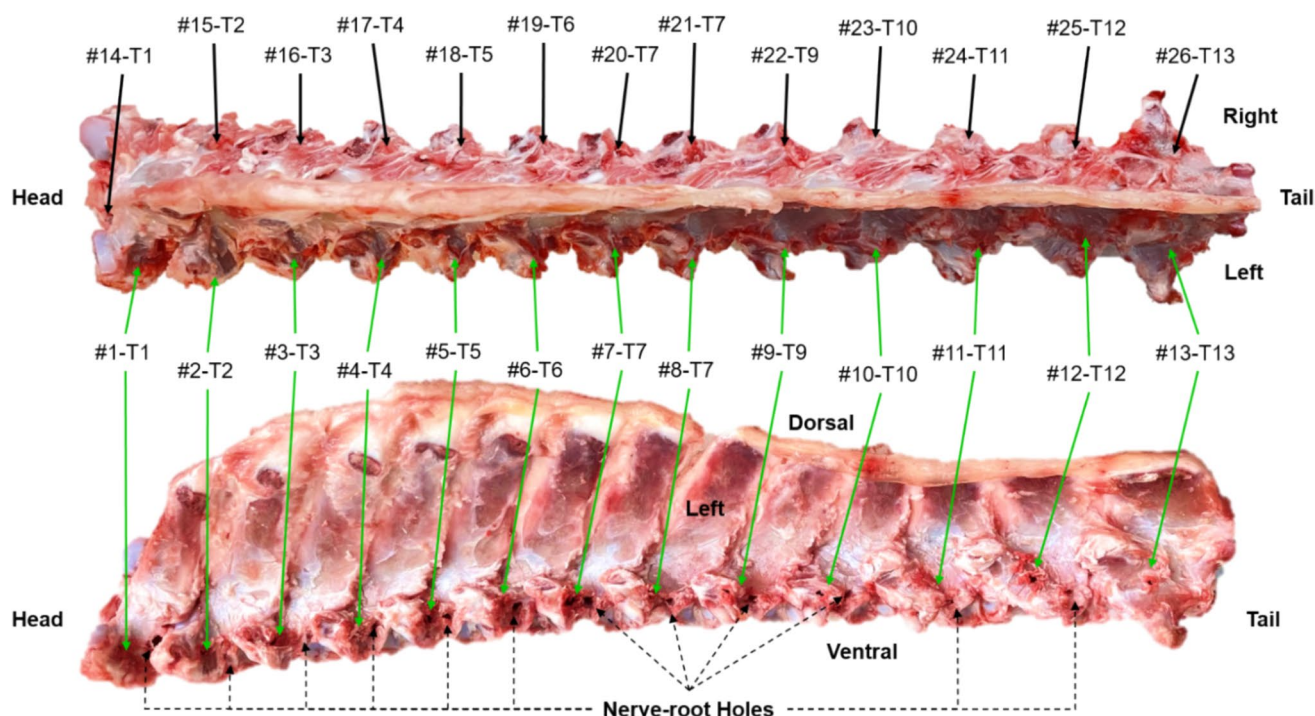


Fig. 1 Fresh caprine thoracic spine and the preparation of pedicle screw holes. The upper part is a dorsal view, and the lower part is a left lateral view. The numbers #1 to #13 correspond to the numberings of the pedicle screw holes on the left side along the head and tail

direction (green arrows), and the numbers #14 to #26 are the numberings on the right side (black arrows). The letter 'T' stands for thoracic vertebrae. The apertures through which the nerve roots pass are pointed by black dashed arrows

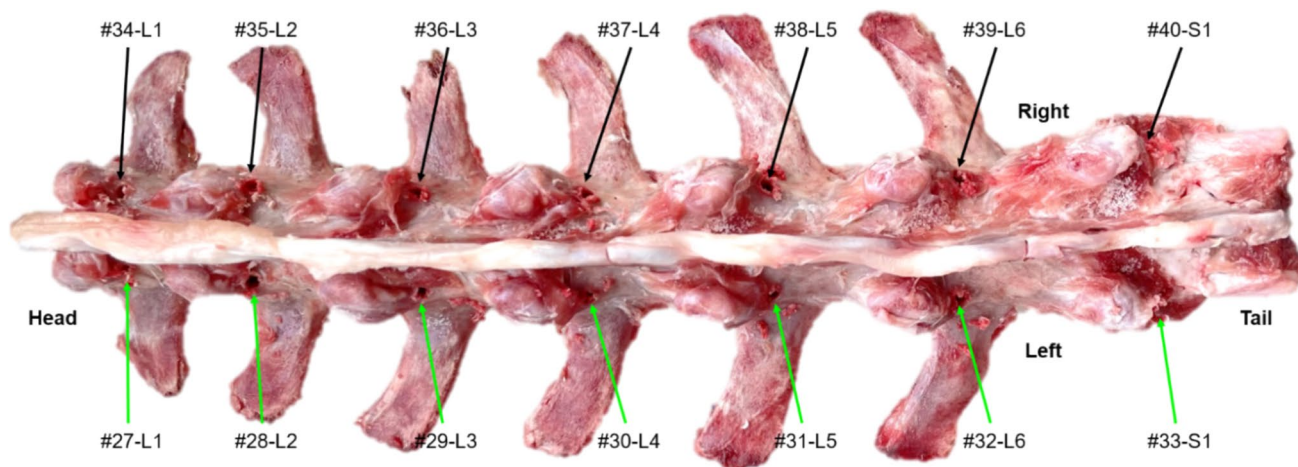


Fig. 2 The dorsal view of fresh caprine lumbar spine and the preparation of pedicle screw holes. The numbers #27 to #33 correspond to the numberings of the pedicle screw holes on the left side along the

head and tail direction (green arrows), and the numbers #34 to #40 are the numberings on the right side (black arrows). The letter 'L' and 'S' represent the lumbar and sacral vertebrae, respectively

2). Of these, a small number of screw holes were established along the presumed correct trajectory, while the majority of holes were intentionally positioned to deviate to the inward side of the pedicles or to directly penetrate the cortex into the spinal canal.

Ultrasound imaging

The EUS mini probe system chose the Jupiter system (Sonoscape, Shenzhen, China) which combines a console with model EU10 and a controller with model TP10,

equipped with a probe with model UM2412 (Sonoscape, Shenzhen, China). The probe has a maximum outer diameter of 2.4 mm and operates at a frequency of 12 MHz. The ultrasound transducer of this probe is embedded on the lateral direction of the tip, providing real-time 360° 2D transverse section images relative to the long axis of probe (Fig. 3). During the ultrasonography process, the specimen was constantly immersed in 0.9% saline solution. When capturing consistent dynamic images, the probe was retracted at a constant speed from the bottom of the pedicle screw holes to the entry-point, acquiring approximately 120–180 frames for each hole. Finally, the dynamic images were exported and saved as DICOM format. Then a DICOM conversion software was employed to extract the images for analysis from the above images in the ratio of 1 out of 10 (about 1 mm apart) and to convert them to TIFF format for visualization and interpretation. All ultrasound

images were interpreted by three independent reviewers (including two spinal surgeons and one sonographer) who had no prior experience in IOUS and were also unaware of the actual positions of the screw holes and the results of CT.

CT scan

The spinal specimen was scanned by a 128-slice spiral CT scanner (UCT760, United Imaging Healthcare, Shanghai, China) according to the following protocol: unenhanced helical acquisition with 120 kV, 0.6 s rotation speed, 4 mm collimation width, and a pitch of 0.9875. Images reconstructed with 1.0 mm thickness at a 0.625 mm intervals. After obtaining the CT images, the results of the ultrasound and CT were compared.

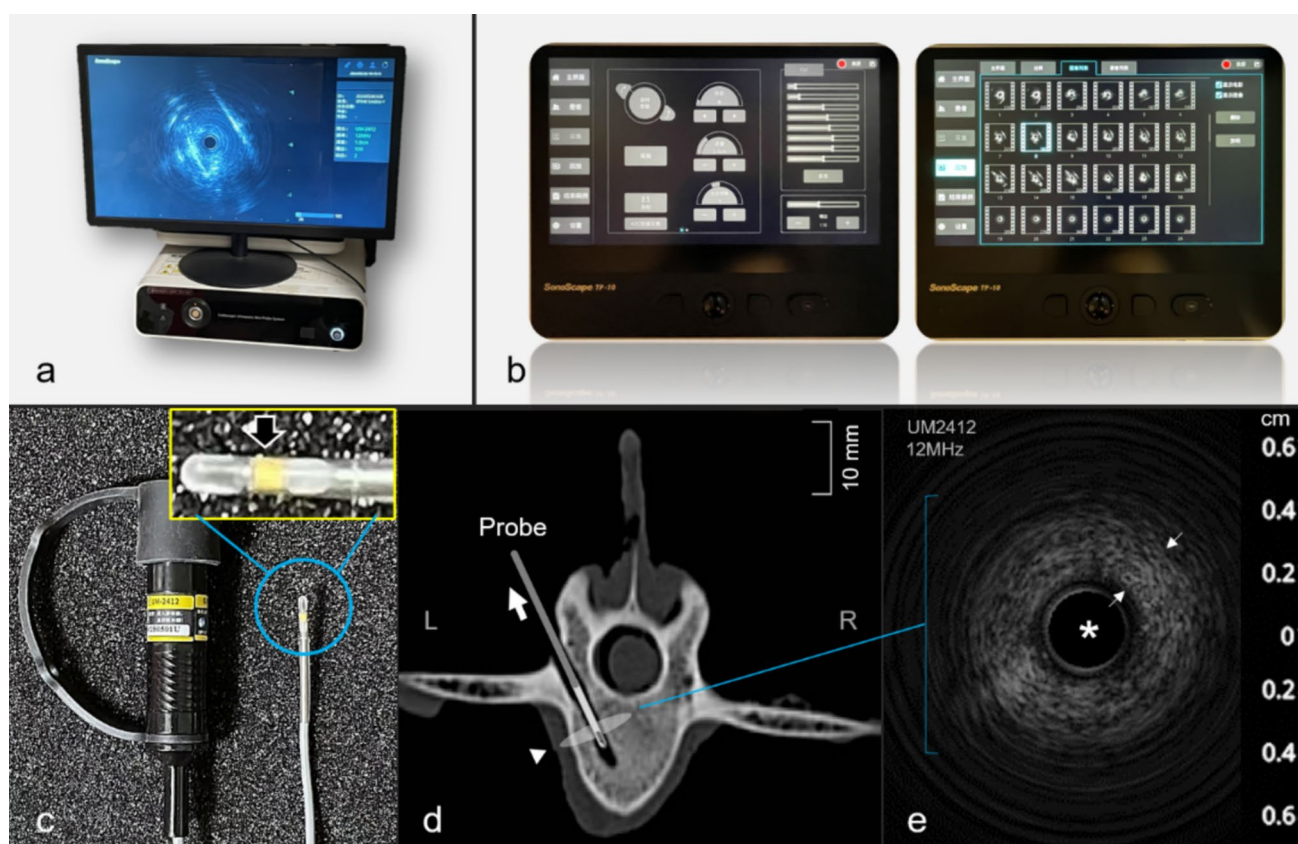


Fig. 3 Jupiter EUS mini probe system and IOUS imaging of pedicle screw holes based on EUS. (a) LCD monitor and the model EU10 console of Jupiter system responsible for the transmission, reception and processing of ultrasonic signals. (b) The model TP10 controller of Jupiter system responsible for the acquisition, storage, management, and post-processing of image data. (c) A probe with model UM2412 and the transducer at the tip of the probe that is magnified and displayed (black arrow). (d) The illustration of the imaging

modality of the mini probe of EUS placed inside the pedicle screw hole: a 2D 360° IOUS imaging of the screw hole was achieved during the retracted process of the probe (a thick white arrow indicates the direction of retraction and a white triangle mark indicates the transverse section image by ultrasound scanning). (e) The EUS image in a screw hole: the probe (white asterisk) located in the center of the image and the wide ring-like echo outside of the screw hole wall (thin white arrow points to)

Accuracy of assessment of pedicle screw holes

The degree of malposition of the pedicle screw holes were classified used the 2 mm increment according to the extent of screw hole deviation shown in CT images [1, 6]: (1) Correct position, if the screw hole is completely within the pedicle and there is no cortex damage; (2) Minor malposition, if the screw hole deviation is < 2 mm (Fig. 4a); (3) Moderate malposition, if the screw hole deviation is ≥ 2 mm but < 4 mm (Fig. 4b); (4) Severe malposition, if the screw hole deviation is ≥ 4 mm (Fig. 4c) or the cortex is penetrated causing the screw hole entirely inside the spinal canal (Fig. 4d). The clinical significance of more than 2 mm deviation lies in the fact that an intraoperative correction of the screw hole trajectory or screw revision should be required.

Statistical analysis

A χ^2 test was performed to conduct non-parametric analysis on the relationship between interpretations of EUS images and reviewers, as well as the relationship between the interpretation for malposition of screw holes and imaging methods. The significance level for testing was set at 95% ($P = 0.05$ threshold).

Results

In the 76 pedicle screw holes, CT reveal that there were 13 holes (17.11%) with correct position, while there were a total of 63 holes (82.89%) with malposition. Among the

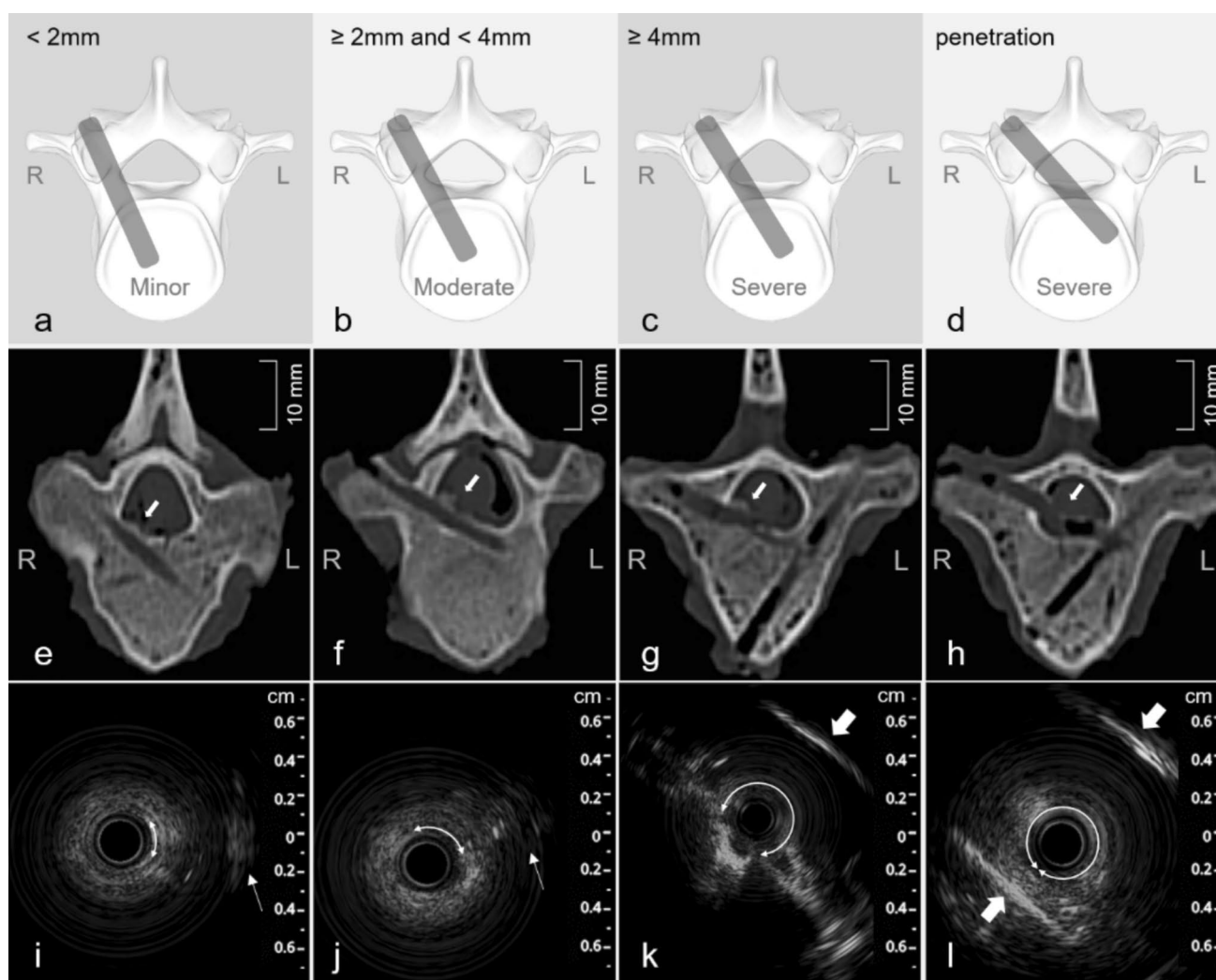


Fig. 4 From top to bottom, the schematic, CT, and EUS images of different degrees of pedicle screw hole malposition are shown, respectively. From left to right, the degree of malposition is minor, moderate, severe without penetration, and severe with penetration. The white arrows within the image (e) to (h) point to the breaches

of screw holes. The arcs with arrows at both ends indicate the absent range of the screw hole wall. The white thin arrows indicate echoes from the tissues out of the hole in the image (i) and (j), and the white thick arrows indicate the walls of the spinal canal in the image (k) and (l)

misplaced holes, there were 9 holes (11.84%) with minor malposition, 9 holes (11.84%) with moderate malposition, 45 holes (59.21%) with severe malposition (Including 35 holes where the spinal canal was penetrated) (Fig. 4e-h).

The black anechoic area at the center of the EUS images was the space occupied by the ultrasound probe, bordered by a white slender ring (Fig. 3c). The echo's blind zone just outside the border was approximately 0.25 mm width. Since the diameter of the screw holes established by the pneumatic drill was 3 mm, which just accommodated the EUS probe with an outer diameter of 2.4 mm. There was almost no display of the lumen echo between the screw hole and the probe (Fig. 5b-h). This was distinct from the obvious lumen echoes between the screw holes prepared with 5.5 mm diameter tap by Kantelhardt SR. and the IVUS catheter with 1.2 mm diameter [7, 8]. In our study, the same phenomena can also exit when a probe model UM1720 (SonoScape, Shenzhen, China) with 1.7 mm diameter and 20 MHz frequency was placed in the pedicle screw holes.

Against the grading criteria of screw hole malposition based on CT, the ultrasound findings were as follows: (1) When the position of the screw hole was correct and entirely within the pedicles, the echo around the hole appeared as an intact wide ring-like structure composed of diffused coarse speckles with medium intensity, and the average ring width was of about 2 mm (Figs. 3c and 5b-h). (2) When the malposition of the hole was minor to moderate, the site of damaged cortex in the wide ring structure showed the focal deformation or absence accompanied by varying degrees of echo from surrounding tissues (Fig. 4 i, j). However, the damaged area may sometimes also show a slightly enhanced echoes. (3) In the images with severe screw hole malposition, the ultrasound presentation is characterized by the absence of the most of the wide ring, even the disappearance of the echo of the spinal canal wall on the same side, accompanied by the appearance of the echo of the spinal canal wall on the opposite side (Figs. 4k and 5m-p). (4) When the screw holes completely penetrate through the pedicle cortex into the spinal canal, the ultrasound images manifest as the whole loss

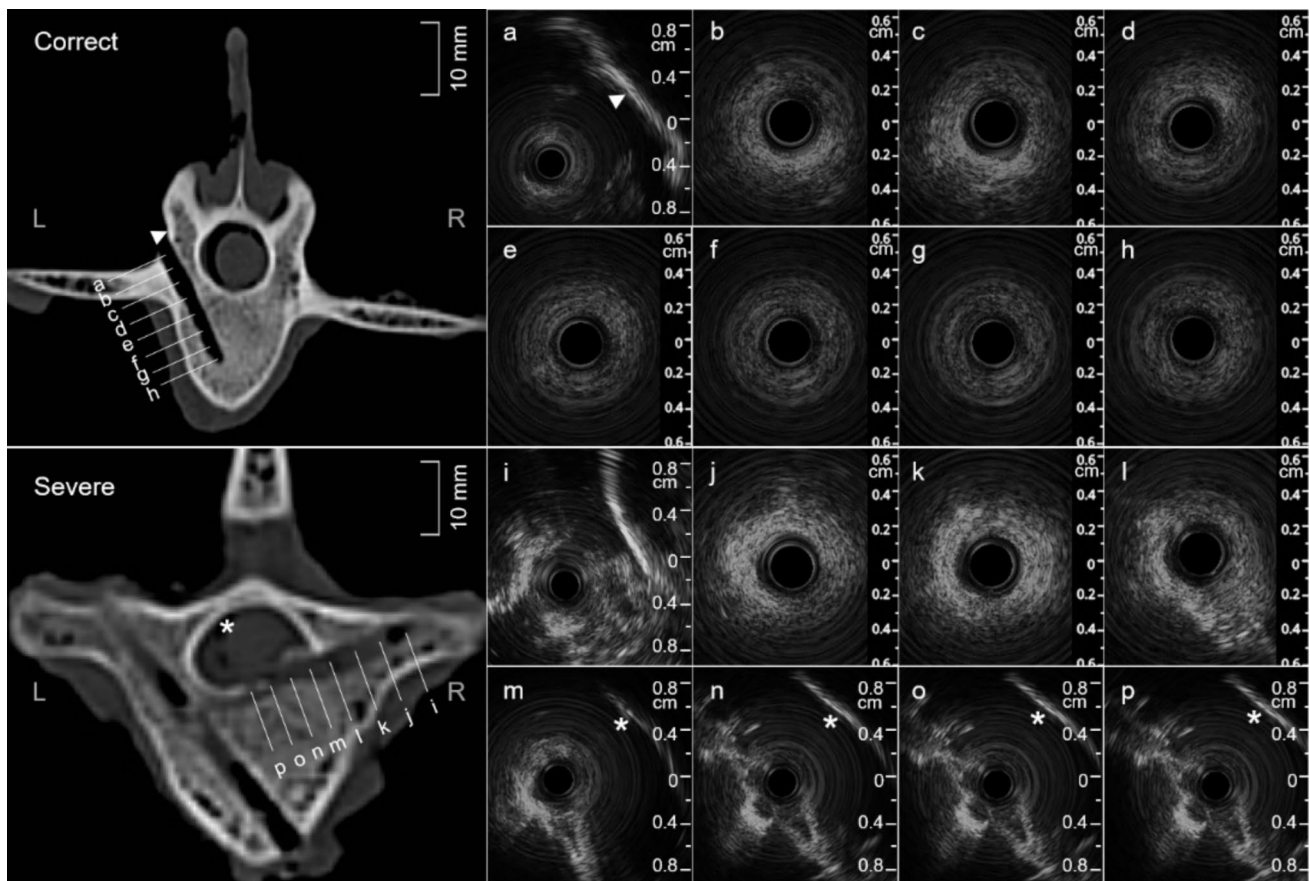


Fig. 5 The EUS images of pedicle screw holes with correct position and severe malposition. (a) to (h) represent the ultrasound images at different depth positions from the entry-point to the bottom in the correctly positioned screw hole. The linear strong echo represents the lamina (triangle mark). (i) to (p) represent the ultrasound images

at different depth positions from the entry-point to the bottom in the screw hole determined to be severe malposition. The CT image in the lower corner shows that the screw hole has partially breached into the spinal canal. In the corresponding EUS image, the opposite wall (white asterisk) of the spinal canal can be detected

of wide ring echo, replaced by linear, high-intensity echoes from the walls of the spinal canal on both sides of the screw hole (Fig. 4 l).

In addition, there were also three types of ultrasound images cannot be easily classified according to the standards of CT. Their ultrasound manifestations are as follows: (1) The suspicious slight malposition. In EUS images, although the wide ring echo remains intact and shows no significant deformation, there is an enhancement of the local echo on the side of the spinal canal (Fig. 6a-c). In contrast, in CT images, it can be observed that the screw hole is completely located within the pedicle, but the wall of the hole is adjacent to the wall of the spinal canal, with only a thin layer of pedicle cortex between them; (2) The malposition with the degree from moderate to severe. In EUS images, despite the

echo from the contralateral spinal canal wall is reflected, the absence or deformation of the wide ring echo is not obvious, making it difficult for inexperienced reviewers to accurately distinguish the degree of malposition (Fig. 6d-f). (3) The characteristic suspicious malposition. In EUS images, on both sides of the wide ring echo, a finger-like protruding structure similar to the wall of a canal, with high intensity echo, appears in sequence. Inside it, there is low or no echo (Fig. 6g,h). The suspicious structures were confirmed by CT as the intersections of bilateral pedicle screw holes, but were all mistakenly concluded as positive results by the 3 reviewers.

The ultrasonic examination time for each pedicle screw hole, from pushing the probe to the bottom end of the hole to fully withdrawing from the pedicle, is approximately 15 s.

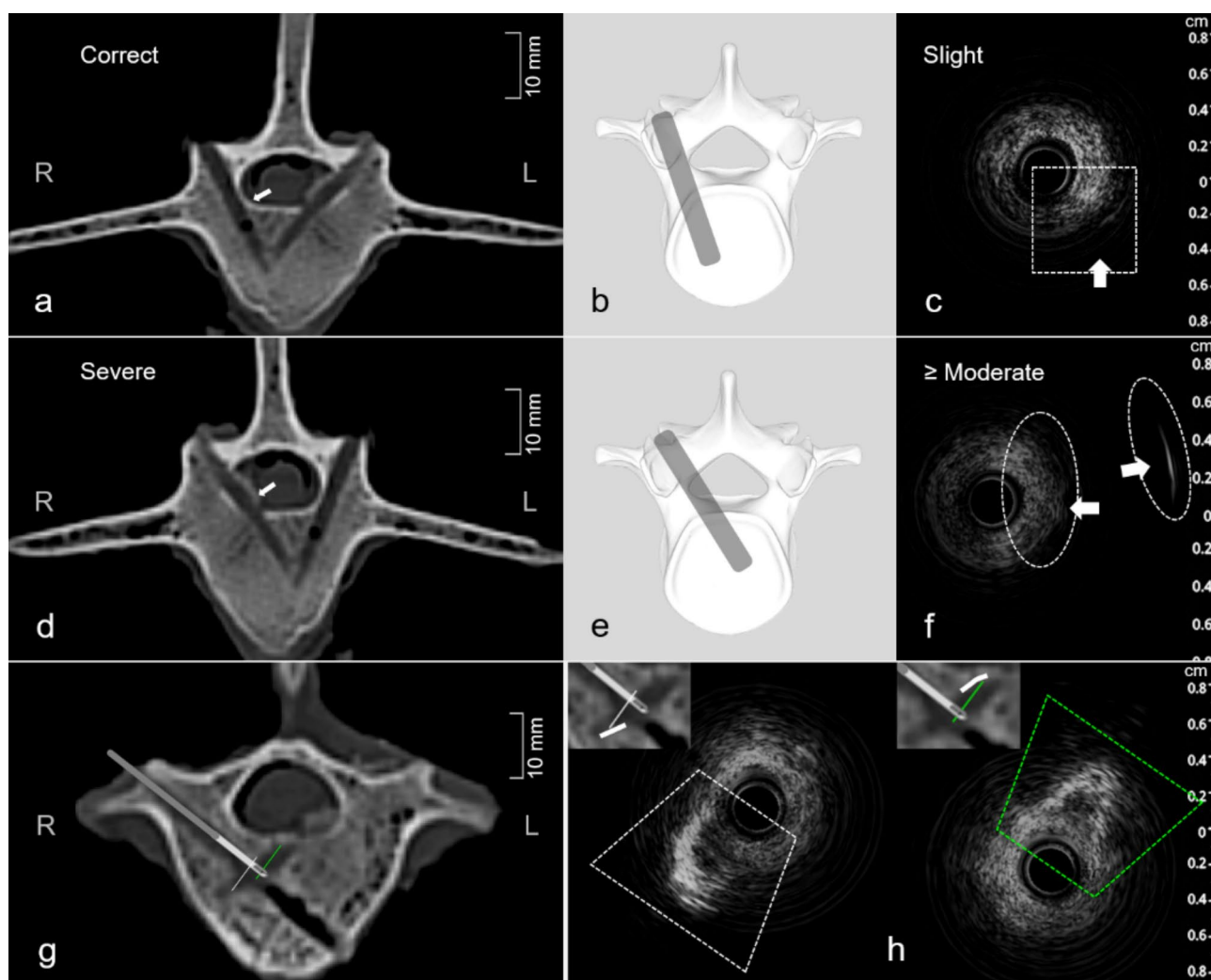


Fig. 6 Three special types of screw hole malposition. (a) to (c), The screw hole shown by CT as being in the correct position was identified by IOUS as slight malposition (white box). (d) to (f), The screw hole shown by CT as a severe malposition was identified by IOUS as a moderate-to-severe malposition (white elliptic frame). (g) and (h),

The finger-like echoes detected in one of the screw holes close to the intersection of the two screw holes and appeared at the both sides of the wide ring are actually the wall of another screw hole located in the same vertebra (white and green trapezoidal frame). The detected hole wall on one side is indicated by a thick white line

After introducing the correct ultrasonic manifestations of screw hole positions, blinded analysis of ultrasonic data from 76 groups of screw holes by 3 independent reviewers showed that there was no significant difference in the correct interpretation of EUS images among reviewers (Fig. 7a), and all malpositions were identified (including six false-positive results). Two additional individuals (one out of the two surgeons and the sonographer) believe that there is a possibility of slight malposition in four screw holes judged to be correctly positioned by CT. Furthermore, after a simple explanation and training regarding the characteristic suspicious malposition for all reviewers, these false positives can be easily identified. It is not difficult to observe from the statistical chart that, after excluding the impact of false positive samples, there is no difference between the subjective interpretation of ultrasound and the objective determination of CT regarding the presence or absence of malposition in the screw holes (Fig. 7 b, c).

Discussion

In this study, we provide for the first time experimental data on the feasibility, sensitivity, and reliability of EUS for IOUS assessment within the pedicle screw holes. The experimental materials consist of fresh caprine thoracolumbar spine, which have biomechanical properties highly similar to those of humans. In the experimental setting, we prepare the pedicle screw holes using the same instruments for spinal surgery. A blinded assessment comparing EUS images and CT images indicates that IOUS based on EUS is highly reliable for monitoring the malposition of pedicle screw holes or cortical breaches. Moreover, researchers, regardless of their experience with ultrasound, can comfortably and correctly interpret the IOUS images of screw holes after a brief

training, demonstrating good intuitiveness and repeatability, with no false-negative results. Additionally, the tip of the EUS probe possesses both flexibility and a characteristic that makes it not easily bent, which is particularly suitable for intraoperative IOUS and percutaneous MISS.

In terms of interpreting images from IOUS of the pedicle screw holes, the frequency of the EUS probe is lower than that of the IVUS ultrasound probe (12 MHz vs. 20 MHz), which gives the EUS probe greater penetrating power. Consequently, the echoes around the screw holes will appear as a wide ring structure, differing from the thin ring-like structure seen with IVUS. In addition, since the screw holes are located within the cancellous bone of the pedicle or the vertebral body, and the attenuation of ultrasound in cancellous bone is significantly lower than in cortical bone, as well as the presence of gaps among the rich trabecular structures within the cancellous bone, the echo of the cancellous bone surrounding the hole appears as a wide ring image with a diffuse dot-line texture. Sometimes, when the screw hole is minor malposition, the local echo of the cortex enhances, which may be related to the dura being lifted and the extradural fat covering the damaged holes wall. When the pedicle cortex is slightly damaged, even if CT does not find any signs of dura arching or absence, IOUS may receive a higher echo signal of the dura and extradural fat through the cortex crack, which may explain the suspicious slight malposition observed in the EUS images. In the concurrent branch study, the research team has obtained robust evidence indicating that intraosseous ultrasonography surpasses the gold standard of CT in interpreting slight misplacements of screw holes. Therefore, in this paper, a discussion on the sensitivity and specificity parameters of EUS-based IOUS would be inappropriate. In the ultrasound images with false positives, the strong echo edge of the finger-like structure is actually the echo of the contralateral pedicle screw hole

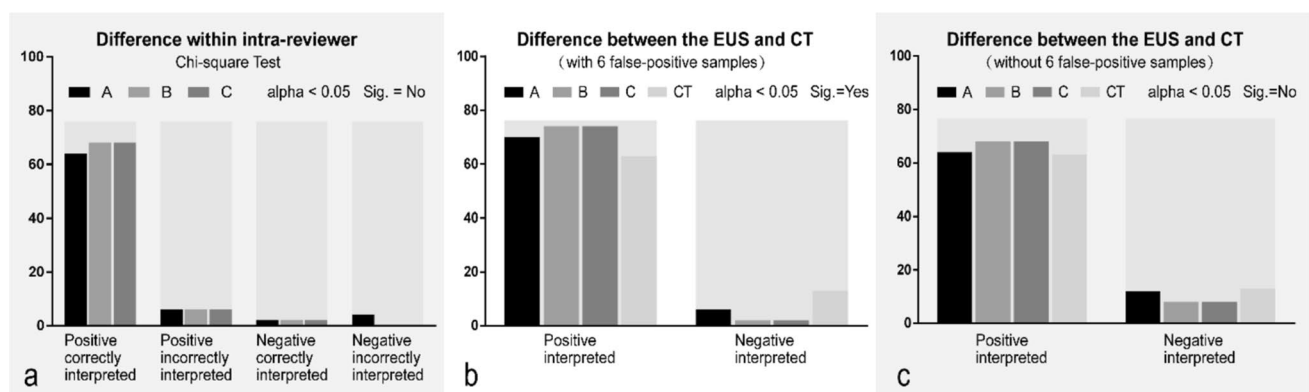


Fig. 7 The non-parametric analysis of the relationship between the interpretation of screw hole malposition in the EUS images and the reviewers or imaging methods. 3 reviewers are represented by A, B, and C respectively. **(a)** The interpretation of pedicle screw hole

malposition among reviewers is without difference. **(b)** and **(c)** The discrepancies in interpretation regarding the screw hole malposition between the EUS and CT images were eliminated after excluding false-positive samples

wall, which is filled with anechoic saline solution. This phenomenon of enhanced edge echo is caused by an ultrasound artifact known as the rear echo enhancement effect.

Strengths and limitations

Currently, screw insertion still relies primarily on free-hand technique based on tactile feedback, which require a high level of surgical skill, are time-consuming, and are prone to human error. Navigation-assisted screw insertion can significantly improve the efficiency and safety of the procedure [11]. Due to advancements in artificial intelligence, robotics, and advanced materials, current intraoperative navigation technologies are experiencing a phase of explosive development. Image-guided robotic-assisted systems can significantly reduce human errors and surgeon fatigue, while greatly enhancing the success rate of pedicle screw placement [13]. As one of the most "cutting-edge technology" representatives, AR and MR guidance technology can provide surgeons with greater operational flexibility [15]. However, these technologies currently do not have an effective strategy to address the registration misalignment caused by patient movement during surgery. The EUS-based IOUS technique eliminates the need for cumbersome registration, while offering high flexibility and being radiation-free. It can be regarded as an auxiliary assessment and guidance technology in the process of pedicle screw navigation. Given the surgeon's solid anatomical knowledge and the intuitive nature of ultrasound imaging, the learning curve for IOUS inherently holds an advantage over navigation systems that are theoretically and operationally complex. Despite this, the attenuation of ultrasound and the lack of ultra-high resolution prevent this technology from serving as an independent alternative guidance method. With breakthroughs in material technology and the introduction of micro-flow detection techniques into miniature probes, the clinical application prospects of IOUS are highly promising.

Conclusion

This experimental research has found that IOUS based on EUS is a potentially low-cost and easy-to-operate, easy-to-interpret, and repeatable technology for verification of pedicle screw malposition and its degree in real-time during the surgery. A recent research hotspot focuses on integrating a mini ultrasound transducer at the tip of the drill to achieve the function of drilling and detecting simultaneously. In the near future, this improvement may enable early warning of pedicle malposition, allow for timely intraoperative correction of the screw trajectory, and significantly reduce the incidence of severe malposition and spinal cord injury. The

clinical significance of this experimental study is to have proved the validity and reliability of experimental data, providing a theoretical basis and practical foundation for the upcoming innovation.

Authors' contributions Y.D. and X.C. contributed to the study conception and design. Material and all figures preparation, EUS images collection and data analysis were performed by Y.D.. CT scanning was performed by X.Z.. The interpretations of the EUS images were finished by H.S., H.W. and S.H.. The main manuscript text was written by Y.D.. X.C. and J.X. were responsible for writing-review and supervision. All authors read and approved the final manuscript.

Funding This work was supported by the National Natural Science Foundation of China (Grant No. 81871470); Multi-center clinical study on standardized comprehensive diagnosis and treatment of pathological fractures, China (Grant No. 23Y31900200); Top priority research center construction project approved by Shanghai Municipal Health Commission, China (Grant No. 2022ZZ01013); The project of orthopedic clinical medical research center construction approved by The Science and Technology Commission of Shanghai Municipality, China (Grant No. 21MC1930100).

Data availability No datasets were generated or analysed during the current study.

Declarations

Competing interests The authors declare no competing interests.

Open Access This article is licensed under a Creative Commons Attribution-NonCommercial-NoDerivatives 4.0 International License, which permits any non-commercial use, sharing, distribution and reproduction in any medium or format, as long as you give appropriate credit to the original author(s) and the source, provide a link to the Creative Commons licence, and indicate if you modified the licensed material. You do not have permission under this licence to share adapted material derived from this article or parts of it. The images or other third party material in this article are included in the article's Creative Commons licence, unless indicated otherwise in a credit line to the material. If material is not included in the article's Creative Commons licence and your intended use is not permitted by statutory regulation or exceeds the permitted use, you will need to obtain permission directly from the copyright holder. To view a copy of this licence, visit <http://creativecommons.org/licenses/by-nc-nd/4.0/>.

References

1. Allaoui M, Zairi F, Tétard MC, Gaughan J, Chopin D, Assaker R (2018) Contribution of dynamic surgical guidance to the accurate placement of pedicle screws in deformity surgery: a retrospective case series. *World Neurosurg* 120:e466–e471. <https://doi.org/10.1016/j.wneu.2018.08.105>
2. Butler AJ, Colman MW, Lynch J, Phillips FM (2023) Augmented reality in minimally invasive spine surgery: early efficiency and complications of percutaneous pedicle screw instrumentation. *Spine J* 23(1):27–33. <https://doi.org/10.1016/j.spinee.2022.09.008>

3. Buza JA 3rd, Good CR, Lehman RA Jr, et al (2021) Robotic-assisted cortical bone trajectory (CBT) screws using the Mazor X Stealth Edition (MXSE) system: workflow and technical tips for safe and efficient use. *J Robot Surg* 15(1):13–23. <https://doi.org/10.1007/s11701-020-01147-7>
4. Costa F, Villa T, Anasetti F et al (2013) Primary stability of pedicle screws depends on the screw positioning and alignment. *Spine J* 13(12):1934–1939. <https://doi.org/10.1016/j.spinee.2013.03.046>
5. Felix B, Kalatar SB, Moatz B et al (2022) Augmented reality spine surgery navigation: increasing pedicle screw insertion accuracy for both open and minimally invasive spine surgeries. *Spine (Phila Pa 1976)* 47(12):865–872. <https://doi.org/10.1097/BRS.0000000000004338>
6. Gueziri HE, Georgiopoulos M, Santaguida C, Collins DL (2022) Ultrasound-based navigated pedicle screw insertion without intraoperative radiation: feasibility study on porcine cadavers. *Spine J* 22(8):1408–1417. <https://doi.org/10.1016/j.spinee.2022.04.014>
7. Kantelhardt SR, Bock CH, Larsen J et al (2009) Intraosseous ultrasound in the placement of pedicle screws in the lumbar spine. (*Phila Pa 1976*) 34(4):400–407. <https://doi.org/10.1097/BRS.0b013e31819286ca>
8. Kantelhardt SR, Bock HC, Siam L et al (2010) Intra-osseous ultrasound for pedicle screw positioning in the subaxial cervical spine: an experimental study. *Acta Neurochir (Wien)* 152(4):655–661. <https://doi.org/10.1007/s00701-009-0447-6>
9. La Rocca G, Mazzucchi E, Pignotti F et al (2022) Intraoperative CT-guided navigation versus fluoroscopy for percutaneous pedicle screw placement in 192 patients: a comparative analysis. *J Orthop Traumatol* 23(1):44. <https://doi.org/10.1186/s10195-022-00661-8>
10. Lashkari B, Mandelis A (2014) Coregistered photoacoustic and ultrasonic signatures of early bone density variations. *J Biomed Opt* 19(3):36015. <https://doi.org/10.1117/1.JBO.19.3.036015>
11. Mandelka E, Gierse J, Zimmermann F, Gruetzner PA, Franke J, Vetter SY (2023) Implications of navigation in thoracolumbar pedicle screw placement on screw accuracy and screw diameter/pedicle width ratio. *Brain Spine* 11(3):101780. <https://doi.org/10.1016/j.bas.2023.101780>
12. Morse KW, Otremski H, Page K, Widmann RF (2021) Less invasive pediatric spinal deformity surgery: the case for robotic-assisted placement of pedicle screws. *HSS J* 17(3):317–325. <https://doi.org/10.1177/15563316211027828>
13. Motov S, Butenschoen VM, Krauss PE, Veeravagu A, Yoo KH, Stengel FC, Hejrati N, Stienen MN (2024) Current state and future perspectives of spinal navigation and robotics-an AO spine survey. *Brain Spine* 18(5):104165. <https://doi.org/10.1016/j.bas.2024.104165>
14. Oh JY (2024) Commentary on “A propensity score-matched cohort study comparing 3 different spine pedicle screw fixation methods: freehand, fluoroscopy-guided, and robot-assisted techniques.” *Neurospine* 21(1):95–96. <https://doi.org/10.14245/ns.2448240.120>
15. Reinhold M, Asal C, Driesen T, Roch J, Jäckle K, Borgmann S, Lehmann W (2024) Learning effectiveness of clinical anatomy and practical spine surgery skills using a new VR-based training platform. *Brain Spine* 10(4):102826. <https://doi.org/10.1016/j.bas.2024.102826>
16. Saad M, Tonetti J, Kerschbaumer G, Boudissa M (2024) Navigated pedicle screw insertion with the Surgivisio system: malposition rate and risk factors - about 648 screws. *Orthop Traumatol Surg Res* 25:103899. <https://doi.org/10.1016/j.otsr.2024.103899>
17. Shubert J, Lediju Bell MA (2018) Photoacoustic imaging of a human vertebra: implications for guiding spinal fusion surgeries. *Phys Med Biol* 63(14):144001. <https://doi.org/10.1088/1361-6560/aacdd3>
18. Spirig JM, Golshani S, Farshad-Amacker NA, Farshad M (2021) Patient-specific template-guided versus standard freehand lumbar pedicle screw implantation: a randomized controlled trial. *J Neurosurg Spine* 35(2):147–153. <https://doi.org/10.3171/2020.10.SPINE201383>
19. Staartjes VE, Klukowska AM, Schröder ML (2018) Pedicle screw revision in robot-guided, navigated, and freehand thoracolumbar instrumentation: a systematic review and meta-analysis. *World Neurosurg* 116:433–443.e8. <https://doi.org/10.1016/j.wneu.2018.05.159>

Publisher's Note Springer Nature remains neutral with regard to jurisdictional claims in published maps and institutional affiliations.